2-6-2012

Spin-Labeling Magnetic Resonance Imaging Detects Increased Myocardial Blood Flow After Endothelial Cell Transplantation in the Infarcted Heart

HuaLei Zhang
University of Pennsylvania

Hui Qiao

Rachel S. Frank

Bin Huang

Kathleen J. Propert

See next page for additional authors

Recommended Citation

Zhang, H., Qiao, H., Frank, R. S., Huang, B., Propert, K. J., Margulies, S. S., Ferrari, V. A., Epstein, J. A., & Zhou, R. (2012). Spin-Labeling Magnetic Resonance Imaging Detects Increased Myocardial Blood Flow After Endothelial Cell Transplantation in the Infarcted Heart. *Circulation: Cardiovascular Imaging*, *5* (2), 210-217. http://dx.doi.org/10.1161/CIRCIMAGING.111.966317

Spin-Labeling Magnetic Resonance Imaging Detects Increased Myocardial Blood Flow After Endothelial Cell Transplantation in the Infarcted Heart

Abstract

Background

We quantified absolute myocardial blood flow (MBF) using a spin-labeling MRI (SL-MRI) method after transplantation of endothelial cells (ECs) into the infarcted heart. Our aims were to study the temporal changes in MBF in response to EC transplantation and to compare regional MBF with contractile function (wall motion) and microvascular density.

Methods and Result

We first validated the SL-MRI method with the standard microsphere technique in normal rats. We then induced myocardial infarction in athymic rats and injected 5 million ECs (human umbilical vein endothelial cells) suspended in Matrigel or Matrigel alone (vehicle) along the border of the blanched infarcted area. At 2 weeks after myocardial infarction, MBF averaged over the entire slice (P=0.038) and in the infarcted region (P=0.0086) was significantly higher in EC versus vehicle group; the greater MBF was accompanied by an increase of microvasculature density in the infarcted region (P=0.0105 versus vehicle). At 4 weeks after myocardial infarction, MBF in the remote region was significantly elevated in EC-treated hearts (P=0.0277); this was accompanied by increased wall motion in this region assessed by circumferential strains (P=0.0075). Intraclass correlation coefficients and Bland-Altman plot revealed a good reproducibility of the SL-MRI method.

Conclusion

MBF in free-breathing rats measured by SL-MRI is validated by the standard color microsphere technique. SL-MRI allows quantification of temporal changes of regional MBF in response to EC treatment. The proof-of-principle study indicates that MBF is a unique and sensitive index to evaluate EC-mediated therapy for the infarcted heart.

Keywords

myocardial blood flow, spin-labeling, MRI, myocardial infarction, human umbilical vascular endothelial cells, microspheres, left ventricular ejection fraction

Disciplines

Biomedical Engineering and Bioengineering | Engineering

Author(s)

HuaLei Zhang, Hui Qiao, Rachel S. Frank, Bin Huang, Kathleen J. Propert, Susan S. Margulies, Victor A. Ferrari, Jonathan A. Epstein, and Rong Zhou

Published in final edited form as:
Circ Cardiovasc Imaging. 2012 March 1; 5(2): 210–217. doi:10.1161/CIRCIMAGING.111.966317.

Spin Labeling-MRI Detects Increased Myocardial Blood Flow Post Endothelial Cell Transplantation in the Infarcted Heart

Hualei Zhang, BS[1,2,4,¶], **Hui Qiao, MD, PhD**[1,4,¶], **Rachel S. Frank, BS**[1], **Bin Huang, MD**[1], **Kathleen J. Propert, PhD**[5], **Susan Margulies, PhD**[2], **Victor A. Ferrari, MD**[3,4], **Jonathan A. Epstein, MD**[3,4,6], and **Rong Zhou, PhD**[1,2,4,*]

[1]Laboratories of Molecular Imaging, Department of Radiology, University of Pennsylvania, PA 19104

[2]Department of Bioengineering, University of Pennsylvania, PA 19104

[3]Department of Medicine (Division of Cardiovascular Medicine), University of Pennsylvania, PA 19104

[4]Cardiovascular Institute, University of Pennsylvania, PA 19104

[5]Department of Biostatistics and Epidemiology, University of Pennsylvania, PA 19104

[6]Department of Cell and Developmental Biology, University of Pennsylvania, PA 19104

Abstract

Background—We quantified absolute myocardial blood flow (MBF) using a spin labeling magnetic resonance imaging (SL-MRI) method after transplantation of endothelial cells (ECs) into the infarcted heart. Our aims were to study the temporal changes in MBF in response to EC transplantation, and to compare regional MBF with contractile function (wall motion) and microvascular density.

Methods and Results—We first validated the SL-MRI method with the standard microsphere technique in normal rats. We then induced myocardial infarction (MI) in athymic rats and injected 5-million ECs (human umbilical vein endothelial cells) suspended in Matrigel or Matrigel alone (vehicle) along the border of the blanched infarcted area. At 2-weeks post-MI, MBF averaged over the entire slice ($p = 0.038$) and in the infarcted region ($p = 0.0086$) was significantly higher in EC *vs.* vehicle group; the greater MBF was accompanied by an increase of microvasculature density in the infarcted region ($p = 0.0105$ *vs.* vehicle). At 4-weeks post-MI, MBF in the remote region was significantly elevated in EC-treated hearts ($p = 0.0277$); this was accompanied by increased wall motion in this region assessed by circumferential strains. Intraclass correlation coefficients and Bland-Altman plot revealed a good reproducibility of the SL-MRI method.

Conclusions—Myocardial blood flow in free-breathing rats measured by SL-MRI is validated by the standard color microsphere technique. SL-MRI allows quantification of temporal changes of regional MBF in response to EC treatment. The proof-of-principle study indicates that MBF is a unique and sensitive index to evaluate EC-mediated therapy for the infarcted heart.

[*]Correspondence to: Rong Zhou, PhD, Laboratories of Molecular Imaging, Department of Radiology, University of Pennsylvania, B6 Blockley Hall, 422 Curie Boulevard, Philadelphia, PA 19104, Telephone: 215-746-8747, Fax: 215-573-2113, zhou@rad.upenn.edu.
[¶]Equal contribution authors

Disclosures
None.

Keywords

myocardial blood flow; spin labeling; magnetic resonance imaging; myocardial infarction; human umbilical vascular endothelial cells; microspheres; left ventricular ejection fraction

Quantification of absolute myocardial blood flow (MBF, in units of mL per minute per gram of tissue) is important when evaluating stem cell mediated treatment of myocardial infarction (MI). First, the ability of local blood supply to match metabolic demand of the tissue will affect the survival of grafted cells. Second, new vasculature formed by either transplanted cells or host cells will improve perfusion, which then facilitates graft survival and expansion. Since an increase in capillary density does not necessarily lead to an increase of blood flow *in vivo* [1], a non-invasive quantification of MBF is desirable, and a measurable increase in MBF can be a specific index to determine the success of therapeutic angiogenesis or vasculogenesis in the infarcted heart.

In the REPAIR-AMI clinical trial [2], bone marrow-derived progenitor cells (BMCs) were infused in patients with reperfused acute MI. By measuring blood flow using an intracoronary Doppler probe, the investigators found that the coronary flow reserve (CFR, defined as the ratio of the maximal to the resting coronary blood flow) of infarct-related arteries recovered to a normal level in BMC-treated patients but not in placebo controls. CFR thus provided direct evidence that BMCs restored microvascular function of infarct-related arteries. Microvascular function, quantified by MBF, could be an important predictor of global functional recovery which was achieved in some BMC trials [3] but not in others [4,5]. While BMCs are a mixture of various types of cells, fully differentiated endothelial cells (ECs) [6] or endothelial progenitor cells (EPCs) [7,8] represent a more purified cell population and have been suggested to form new vasculature, preserve LV function and inhibit apoptosis in the infarcted heart. However, mechanisms underlying the salutary effects of these cells are not well understood: specifically, whether or not neovascularization leads to improved regional MBF has not been studied extensively.

To evaluate EC- or EPC-mediated vascular repair over time and to be able to translate it to the clinic, non-invasive imaging based methods for MBF estimation are desirable. At present, positron emission tomography (PET) is the clinical standard for MBF measurement [9]. First-pass contrast-enhanced MRI can be used to *quantify* MBF only after extensive modeling of the kinetic data [10]. In contrast, spin labeling-based magnetic resonance imaging (SL-MRI) utilizes endogenous water molecules, eliminating the need to inject any exogenous tracers. First implemented on the heart by Belle *et al* on the rat *in vivo* [11,12], this technique has proven effective for mapping MBF in rapidly beating rodent hearts to study cardiovascular diseases in such models [13–17].

In this study, first, we validated the SL-MRI method with a standard microsphere technique; second, we utilized SL-MRI to detect changes of MBF over time in the infarcted, border and remote regions in response to EC transplantation, and demonstrated that the improved MBF is corroborated with increased wall motion and microvascular density in the corresponding regions.

Methods

1. Experimental design and study groups

All animal procedures were approved by the local Institutional Animal Care and Use Committee. This study has two aims. Aim-1 is to validate the SL-MRI based MBF

measurement, while Aim-2 is to assess the utility of SL-MRI for detecting MBF changes mediated by EC transplantation in an MI model.

For Aim-1, a total of 18 rats were used; 5 rats completed the study while 13 died during procedures (Section 3). For Aim-2, ECs in the form of human umbilical vein endothelial cells (HUVECs, ATCC, Manassas, VA) were expanded (≤ 6–10 passages) and suspended in growth factor-reduced Matrigel (Collaborative Biomedical, Bedford, MA). MI was induced in male athymic nu/nu rats (6–8 weeks old, Frederick Cancer Center, Frederick, MD) by permanent ligation of the left anterior descending coronary artery [18]. During the same surgical session, 5-million ECs in 100 μl Matrigel, or Matrigel alone (vehicle) were injected in one spot in the border close to the blanched area. Initial infarct size (as a percentage of LV myocardial volume) was assessed at 1 day post-MI using late gadolinium enhancement (LGE), and rats having infarct size outside the range of [10%, 30%] were excluded as we described previously.[18,19] A total of 51 rats (26 were assigned to EC and 25 to Vehicle group) were used in Aim-2; 22 died from surgery and 7 were excluded at Day-1 due to unqualified infarct size; remaining 22 rats (n = 12 in EC and n = 10 in Vehicle group) proceeded to studies at 2-weeks and 4 rats in EC and 3 in Vehicle group were euthanized for microvasculature density (MVD) analysis; the remaining 15 animals were imaged and euthanized at 4-weeks. As the result of instrument downtime, there are missing MBF data from unscanned rats at 1-day and 2-weeks, whereas all rats were scanned at 4-weeks; the number of rats scanned at each time point was specified in figures.

2. SL-MRI based MBF quantification

MR experiments were performed on a 4.7T horizontal bore magnet interfaced to a Varian DirectDrive™ console. A combination of a transverse electro-magnetic (TEM) volume transmit coil and surface receive coil (InsightMRI, Worcester, MA) [18,19] was interfaced to a 12 cm gradient insert with maximum strength of 25G/cm. The rat was maintained under anesthesia by 1.5% (unless indicated otherwise) isoflurane mixed with oxygen at a flow rate of 1L/min via a nose cone. ECG and respiration were monitored (SA Instruments, Stony Brook, NY) and core temperature was maintained at 36.5 ± 0.2°C by warm air. A gel phantom (with relaxation time, T1, slightly longer than normal myocardium) was fixed on the animal holder.

Data acquisition—We modified the SL-MRI protocol by Kober *et al* [20], in which ECG- and respiration-gated gradient echo technique was utilized to achieve high spatial resolution perfusion maps in free-breathing animals. Instead of referencing the phantom with a known T1 to derive tissue T1 values, our protocol directly calculates T1 from a series of inversion recovery images using a least-square fitting algorithm [21,22]. Consequently, the mean perfusion value of the phantom being close to 0 was used as a criterion to evaluate the quality of raw data and T1 fitting.

MBF was measured from a 3-mm short axis slice at mid left ventricle. To map T1 corresponding to non-slice-selective and slice-selective inversion of the magnetization, a modified TOMROP sequence [21,23] was used, which consists of an inversion pulse (followed by crusher gradients) and a gradient echo module that samples the same phase-encoding line multiple times along the magnetization recovery. A hyperbolic secant adiabatic pulse [24] lasting 6–7 ms (permitted by RF coil power limit) was used for the inversion. The slice thickness of the inversion pulse was set to a large value (3×10^5 mm) in the case of global inversion, and to 2.5 times of the imaging slice thickness in the case of slice-selective inversion. The ratio of 2.5 was to compensate the imperfect matching of the inversion and excitation pulse profiles, and was determined using the agarose gel phantom (i.e., under the no-flow condition) by stepwise increasing the ratio of inversion to excitation pulse slice

width as 1, 1.5, 2, 2.5, 3, 3.5 and identifying the smallest inversion pulse slice width that can achieve the “zero” flow results in the phantom.

Immediately after the inversion pulse and under ECG-gating, a series of images were acquired for at least 7-sec followed by a 4-sec delay to ensure that the spins in myocardium were recovered to > 99% of the equilibrium magnetization before the next inversion pulse. The respiratory waveform and k-space acquisitions were simultaneously recorded (SA Instrument, Stony Brook, NY) for retrospective elimination of images acquired outside the quiescent phase of expiration. The following parameters were used: field of view (FOV) = 35 × 35 mm^2, acquisition matrix = 192 × 80, TE = 2.19 ms, bandwidth = 96 kHz, inversion time spacing = 2 heart beats, Gaussian excitation pulse of 800-μs and 10° flip angle; each pair of T1 measurements took about 25 min; 2 signal averages.

Data processing—A three-parameter fitting algorithm [21,22] was used to calculate pixel-wise T1 values under non-slice-selective and slice-selective inversion, designated as $T1_{ns}$ and $T1_{ss}$, respectively. The pixel-wise blood flow was quantified using the formula below [11]:

$$\frac{\mathrm{MBF}}{\lambda}=\frac{\mathrm{T1_{ns}}}{\mathrm{T1_b}}\left(\frac{1}{\mathrm{T1_{ss}}}-\frac{1}{\mathrm{T1_{ns}}}\right), \quad [1]$$

where $\lambda=\frac{\text{quantity of water per gram of tissue}}{\text{quantity of water per gram of blood}}$ is the tissue-blood partition coefficient of water and was set to 0.83 mL/g for rat myocardium. $T1_b$ is the blood T1 under global inversion and was set to 1.6-sec at 200 MHz [11]. The phantom was included for flow calculation (Figure 1A), and an MBF measurement was accepted if the phantom had a mean flow value within ±0.5 mL/min/g; if rejected, the data was reacquired within 2 days of the 2-weeks and 4-weeks time points in the EC study or considered as missing.

3. Validation of SL-MRI based MBF with microsphere method

Before the SL-MRI session, the carotid artery (for direct injection of microspheres into LV) and femoral artery (for withdrawal of reference blood) were cannulated [25]. Placement of the catheter inside LV was verified by proper length of the inserted catheter and rapid blood pulsations in the catheter.

Immediately after SL-MRI, 200,000 fluorescent microspheres (FMs) of 15 μm diameter (Dye-Trak, Triton Technology, San Diego, CA) in 200 μL saline was infused in 10-sec followed by 500 μL saline flush for 20-sec. Meanwhile, reference blood was withdrawn through the femoral artery catheter at 330 μL/min via a syringe pump (Harvard Apparatus, Boston, MA) starting 30-sec before the FM injection and lasting for 180-sec. Upon completion of blood sampling, the heart was harvested and embedded in 1 % agarose gel.

A fluorescent plate/slide imaging protocol [26] was used to quantify the number of FMs. The heart was sectioned into ~100 μm thick sections on a vibratom (Leica VT1000S, Leica Microsystems GmbH, Germany). Sections corresponding to the imaging slice were determined by their positions relative to the apex and mounted on microscope slides. FMs in the reference blood were retrieved by membrane filters, which were also mounted on slides. The slides were then scanned on a fluorescent plate reader (Alpha Innotech, CA). The number of microspheres in slides was counted by a custom program written in MATLAB (Mathworks, Natick, MA). MBF was estimated based on the amount of FMs in the tissue and reference blood as well as thereference blood withdrawal rate[25].

4. Cardiac function post EC transplantation evaluated by MRI

MBF was measured at 1-day, 2- and 4- weeks post-MI, while the infarct size and LVEF [27] was estimated at 1-day and 4-weeks. Regional wall motion was measured at 4-weeks only, from the same slice position as MBF but with 1.5-mm thickness. The MRI protocol for wall motion which was detailed previously [19] was updated to a tag spacing of 0.9-mm (k_e = 1.11 cycle/mm) and 10 cardiac frames (15-ms per frame). To obtain regional MBF and wall motion, LV myocardium was segmented into *I-B-R*, where infarcted (*I*) region was defined on the LGE image (at the same position as MBF slice), border region (*B*) as two 60° sectors on each side of the infarcted segment, and the remote region (*R*) encompassed the remaining myocardium.

5. MVD and incorporation of grafted ECs into vasculature

MVD was estimated at 2- and 4-weeks. Upon euthanasia, a 5-mm thick slab centered at the mid-ventricle level was embedded in Optimal Cutting Temperature media and cut in short axis orientation. After trimming off 1-mm top layer, three sections (each 10-μm thick) were cut at 3 levels with 1-mm spacing. Sections were immunostained using the following antibodies: 1. rabbit polyclonal anti- von Willebrand Factor (vWF) antibody (Sigma, St. Louis, MO) and FITC-conjugated goat anti-rabbit secondary antibody, 2. mouse monoclonal anti-human CD34 antibody (Abcam, Cambridge, MA) and Cy3-conjugated goat anti-mouse secondary antibody. One section at each level was H&E stained.

To estimate regional MVD, each section was segmented into the *I-B-R* region under 2X objective lens: infarcted region was identified on the adjacent H&E section; the border and remote regions were defined in the same way as on MRI. Then under 10X, at least 6 FOVs (each covering 1.1-mm^2) were captured including 3 in the *R*emote, 2 in the *B*order, and 1–3 in the *I*nfarcted region depending on the infarct size. Clustered cells or continuous branching structures with positive vWF staining were counted as one capillary. To visualize engrafted ECs, double immunostaining for human CD34 and vWF was performed.

6. Statistical analyses

Data are presented as mean (± standard deviation) in both text and figures. The Bland-Altman plot and intraclass correlation coefficients (ICC, MedCalc 11.6, Mariakerke, Belgium) calculated from segmental and sliced-averaged MBF were used to evaluate the agreement between MRI- and FM-based MBF measurements. The same approaches were applied to 12 animals (6 in EC and 6 in Vehicle group), each having two serial scans in the same imaging session at 2-weeks post-MI, for assessing the reproducibility of the SL-MRI method. To assess the treatment effect (EC *vs.* Vehicle group), a mixed effect model with repeated measures (PROC MIXED, SAS Institute Inc., Cary, NC) was applied. This model allows inclusion of data from all time points under data missing and evaluates the treatment effect between groups (subjects) and regions (within subject) over time; $p < 0.05$ is considered to be statistically significant.

Results

1. Validation of SL-MRI by microsphere method

In order to validate SL-MRI as a method to accurately measure MBF in living animals, we directly compared SL-MRI measurements to the standard microsphere method in 5 animals: we cannulated the carotid and femoral arteries right before the SL-MRI session, and injected FMs immediately after SL-MRI. MR images were first cropped and the region defined by the blue box (Figure 1A) was processed to derive T1 maps corresponding to non-slice-selective ($T1_{ns}$, Figure 1B) and slice-selective inversion ($T1_{ss}$, Figure 1C). Pixel-wise MBF was calculated by Equation [1] (Figure 1D). MBF was also estimated by counting the

number of FMs in myocardium (one section is shown in Figure 1E). A strong correlation between SL-MRI and FM technique (R = 0.972) was revealed for MBF averaged from the *entire* slice; a slope close to unity suggests an excellent agreement between the two techniques (Figure 1F). To obtain regional MBF measurements, the LV wall on the MBF map and corresponding micrographs was divided into septal, lateral, anterior and posterior quadrants. The anterior and posterior quadrants were combined into one segment since they were not distinguishable on tissue sections. Averaged MBF in the septal, lateral and combined anterior/posterior segments obtained by the two methods remain well-correlated with R value of 0.753 (Figure 1G). A good agreement between the two methods was also demonstrated by the ICC derived from slice-averaged MBF (Table 1) and by Bland-Altman plot (Figure 1H): it revealed a bias of −0.065 mL/min/g, which is not statistically significant from zero ($p = 0.897$), with 95% limits of agreements including all but one data points. To facilitate correlation studies, the percentage of isoflurane applied to individual animals was varied from 1% to 2.5%, since MBF is shown to be regulated by levels of anesthesia.[13] For each animal, however, the percent isoflurane was kept *the same*. The heart and respiration rate were stably maintained during the experiments (Table 2).

2. Changes in regional MBF in response to EC-transplantation

In order to establish the utility of SL-MRI to measure MBF in the setting of EC therapy, we injected ECs or vehicle into the border zone of infarcted hearts and performed serial evaluations over the ensuing 4 weeks. At 1-day post-MI, a relatively uniform infarct size distribution in the two groups was obtained, 18 ± 4.7% in the EC (n = 12) *vs.* 17 ± 5.6% in Vehicle (n = 10) group (Table 3, $p = 0.553$), which facilitated a fair comparison for EC-mediated effects. At 1-day post-MI shown in the inset of Figure 2A, regional MBF was depressed in the infarcted *vs.* remote region. In comparison of slice-averaged MBF over time in EC *vs.* Vehicle group, the MBF is significantly higher in EC group at 2-weeks ($p = 0.0380$). A significant treatment effect on regional MBF was revealed at 2-weeks across regions ($p = 0.0057$) and in the remote region across time points ($p = 0.0402$). When the analysis was refined to specific region or time point, a significant treatment effect in the infarcted region at 2-weeks ($p = 0.0086$) and in the remote region at 4-weeks ($p = 0.0277$) were obtained. Representative MBF maps at 2-weeks indeed show higher MBF in the infarcted segment in the EC- treated heart, which had similar infarct size as the Vehicle-treated one (Figure 2B–E). More capillaries in the infarcted region in EC-treated hearts were revealed by vWF immunostaining (Figure 2F–G); quantitative analysis confirmed a significantly higher MVD in the infarcted region ($p = 0.0105$ EC *vs.* Vehicle group, Figure 2J). Furthermore, double staining for vWF and human CD34 demonstrated incorporation of ECs into capillaries in the infarcted (Figure 2H) and border region (Figure 2I). Taken together, these data provide convincing evidence that EC engraftment enhanced new vessel formation, leading to improved perfusion in the infarcted region detected by SL-MRI.

At 4-weeks post-MI, while MBF in the infarcted region was *no longer* different between the two groups, an elevated MBF in the remote region was detected in EC-treated hearts as visualized in MBF maps from individual rats (Figure 3A–D) and confirmed by statistical analysis ($p = 0.0277$, Figure 3E). Interestingly, elevated MBF was matched by a significant increase (greater absolute values) in circumferential strains (E_{cc}) in the remote region ($p = 0.0075$) as well as E_{cc} averaged over the entire slice ($p = 0.0123$, Figure 3G). The enhanced MBF and E_{cc}, however, did not lead to an increase in LVEF in EC group (Table 3), suggesting that LVEF is not sensitive to detect local changes in perfusion and wall motion. While MVD was greater in all regions of EC-treated hearts, statistical significance was not obtained in any region (Figure 3F). Compared to 1-day post-MI, infarct size decreased in both EC and Vehicle groups (Table 3), likely due to wall thinning in the infarcted region observed frequently in both groups. Compared to 2-weeks post-MI, CD34 positive cells

were rarely found in sections (data not shown) suggesting the vast majority of transplanted cells were dead or removed.

Finally, the SL-MRI method is shown to have a high degree of reproducibility by ICC (Table 1) and by the Bland-Altman plot of regional MBF, which revealed a uniform distribution of differences in MBF (scan2-scan1) around a bias very close to zero (Figure 4). For reproducibility as well as validation study, segment-specific ICC values are relatively low in one or two segments, suggesting a decreased agreement in these segments.

Discussion

HUVECs are commercially available and can be expanded to a large number in vitro, therefore providing a convenient EC source for this proof-of-principle study to examine whether or not SL-MRI is able to detect temporal changes of regional MBF in response to EC engraftment in the infarcted heart. Our results suggest that EC transplantation induces a strong neovascularization response in the infarcted region detectable at 2-weeks post injection, leading to a substantial increase of regional blood flow and capillary density accompanied by incorporation of grafted ECs into capillaries in the infarcted and border regions (Figure 2). The localized responses, although strong, appear to be short-termed and transit to a prominent increase of MBF in the remote territory (Figure 3E). This finding is intriguing because it is generally expected that only infarcted and border zones would benefit from EC engraftment. However, there is compelling evidence that the remote region is affected during unfavorable post-MI remodeling [28] and stem cells may partially rescue/stabilize that region [29]. Consistently, an increase in MBF was accompanied by a recovery of wall motion (E_{cc}) in the remote region.

SL-MRI (also called arterial spin labeling) has achieved a great success in measuring blood flow in the brain [30]. In conventional brain SL, the RF inversion pulse is typically introduced at an upstream location proximal to the tissue of interest. For MBF measurement, however, *on-slice* SL, namely, flow-sensitive alternating inversion recovery (FAIR)[31] technique, can minimize the magnetization transfer artifact and the underestimation of flow when feeding arteries have tortuous paths. SL-based MBF in small rodents is based on T1 mapping and the arterial transit time (ATT) is ignored. This approach might be justified by the fact that small rodents have much higher MBF (3–5 mL/min/g [11,20,32]) than humans (0.7–1 mL/min/g [33]) and are studied at higher field strength than clinical scanners, leading to prolonged blood T1. Therefore, the ATT of un-inverted blood spins is much shorter than blood T1, which allows a measurable inflow effect in slice-selective T1 values [12]. ATT of human heart was estimated at 1.5T recently[34]. While further study is necessary to evaluate the effect of ATT on MBF quantification in small rodents, our validation study suggests the T1 mapping approach is in excellent agreement with standard microsphere method.

While the goals of this study have been fulfilled, several limitations should be discussed. First, compared to the resting MBF, coronary flow reserve, CFR, might be more representative of coronary microvascular function than the resting MBF [35]. CFR measurement can be implemented via pharmacological stimulation in SL-MRI protocol for future studies. Second, single slice MBF was obtained in the current protocol due to relatively lengthy acquisition time (≥ 25 min), which could lead to concerns that MBF may vary during acquisition. Inversion recovery based T1 mapping, while being the most robust method, is inherently time-consuming. Non-Cartesian k-space trajectory such as spiral [16] or radial [36] imaging techniques can reduce acquisition time and resist respiratory motion. Third, due to inflammatory reactions induced by acute MI and/or the use of human cells in a rat model (albeit immune-compromised), injection of ECs during MI surgery might have a negative impact on EC survival. Therefore, better EC engraftment is expected if they are

injected 7 days post-MI as we have shown with embryonic stem cell derived cardiomyocytes.[19] Finally, the high post-surgery mortality rate and the exclusion of 7 rats from the Aim-2 analysis because of unqualified infarct size raise the possibility of selection bias in addition to impacting statistical power.

In summary, our results indicate excellent agreement of MBF in free-breathing rats measured by SL-MRI and the standard color microsphere technique. Non-invasive SL-MRI allows serial assessments of regional MBF in response to EC treatment. The presented method offers a promising framework to quantify MBF as a specific and sensitive index to evaluate EC-mediated therapy for the infarcted heart.

Acknowledgments

We are grateful to Xiaoling Hou, MS, Saran Vardhanabhuti, PhD, and Amy Praestgaard, MS for performing statistical analyses. Special thanks to Dr. Ronald Morris from SA Instrument for modifications of breakout module to allow recordings of respiration waveform with gate bits. We are indebted to Drs. Stephanie Eucker and William M. Armstead for helps with FM protocol. We thank Dr. Jifu Yang for tissue sectioning and the Small Animal Imaging Facility (SAIF) for technical support.

Sources of Funding

NIH grants R01-HL081185A1 and R01-HL081185S1 (RZ).

References

1. Chiu RC. Therapeutic cardiac angiogenesis and myogenesis: the promises and challenges on a new frontier. J Thorac Cardiovasc Surg. 2001; 122:851–2. [PubMed: 11689786]
2. Erbs S, Linke A, Schachinger V, Assmus B, Thiele H, Diederich K-W, Hoffmann C, Dimmeler S, Tonn T, Hambrecht R, Zeiher AM, Schuler G. Restoration of Microvascular Function in the Infarct-Related Artery by Intracoronary Transplantation of Bone Marrow Progenitor Cells in Patients With Acute Myocardial Infarction: The Doppler Substudy of the Reinfusion of Enriched Progenitor Cells and Infarct Remodeling in Acute Myocardial Infarction (REPAIR-AMI) Trial. Circulation. 2007; 116:366–374. [PubMed: 17620510]
3. Schachinger V, Assmus B, Erbs S, Elsasser A, Haberbosch W, Hambrecht R, Yu J, Corti R, Mathey DG, Hamm CW, Tonn T, Dimmeler S, Zeiher AM. Intracoronary infusion of bone marrow-derived mononuclear cells abrogates adverse left ventricular remodelling post-acute myocardial infarction: insights from the reinfusion of enriched progenitor cells and infarct remodelling in acute myocardial infarction (REPAIR-AMI) trial. European Journal of Heart Failure. 2009; 11:973–979. [PubMed: 19789401]
4. Janssens S, Dubois C, Bogaert J, Theunissen K, Deroose C, Desmet W, Kalantzi M, Herbots L, Sinnaeve P, Dens J, Maertens J, Rademakers F, Dymarkowski S, Gheysens O, Van Cleemput J, Bormans G, Nuyts J, Belmans A, Mortelmans L, Boogaerts M, Van de Werf F. Autologous bone marrow-derived stem-cell transfer in patients with ST-segment elevation myocardial infarction: double-blind, randomised controlled trial. Lancet. 2006; 367:113–21. [PubMed: 16413875]
5. Lunde K, Solheim S, Aakhus S, Arnesen H, Abdelnoor M, Egeland T, Endresen K, Ilebekk A, Mangschau A, Fjeld JG, Smith HJ, Taraldsrud E, Grogaard HK, Bjornerheim R, Brekke M, Muller C, Hopp E, Ragnarsson A, Brinchmann JE, Forfang K. Intracoronary injection of mononuclear bone marrow cells in acute myocardial infarction. N Engl J Med. 2006; 355:1199–209. [PubMed: 16990383]
6. Nishiyama K, Takaji K, Kataoka K, Kurihara Y, Yoshimura M, Kato A, Ogawa H, Kurihara H. Id1 Gene Transfer Confers Angiogenic Property on Fully Differentiated Endothelial Cells and Contributes to Therapeutic Angiogenesis. Circulation. 2005; 112:2840–2850. [PubMed: 16267257]
7. Kawamoto A, Iwasaki H, Kusano K, Murayama T, Oyamada A, Silver M, Hulbert C, Gavin M, Hanley A, Ma H, Kearney M, Zak V, Asahara T, Losordo DW. CD34-Positive Cells Exhibit Increased Potency and Safety for Therapeutic Neovascularization After Myocardial Infarction Compared With Total Mononuclear Cells. Circulation. 2006; 114:2163–2169. [PubMed: 17075009]

8. Li Z, Wu JC, Sheikh AY, Kraft D, Cao F, Xie X, Patel M, Gambhir SS, Robbins RC, Cooke JP, Wu JC. Differentiation, Survival, and Function of Embryonic Stem Cell Derived Endothelial Cells for Ischemic Heart Disease. Circulation. 2007; 116:I-46–54. [PubMed: 17846325]
9. Di Carli MF, Hachamovitch R. New Technology for Noninvasive Evaluation of Coronary Artery Disease. Circulation. 2007; 115:1464–1480. [PubMed: 17372188]
10. Li X, Springer CS Jr, Jerosch-Herold M. First-pass dynamic contrast-enhanced MRI with extravasating contrast reagent: evidence for human myocardial capillary recruitment in adenosine-induced hyperemia. NMR Biomed. 2009; 22:148–57. [PubMed: 18727151]
11. Belle V, Kahler E, Waller C, Rommel E, Voll S, Hiller KH, Bauer WR, Haase A. In vivo quantitative mapping of cardiac perfusion in rats using a noninvasive MR spin-labeling method. J Magn Reson Imaging. 1998; 8:1240–5. [PubMed: 9848735]
12. Bauer WR, Hiller KH, Roder F, Rommel E, Ertl G, Haase A. Magnetization exchange in capillaries by microcirculation affects diffusion-controlled spin-relaxation: a model which describes the effect of perfusion on relaxation enhancement by intravascular contrast agents. Magn Reson Med. 1996; 35:43–55. [PubMed: 8771021]
13. Kober F, Iltis I, Cozzone PJ, Bernard M. Myocardial blood flow mapping in mice using high-resolution spin labeling magnetic resonance imaging: influence of ketamine/xylazine and isoflurane anesthesia. Magn Reson Med. 2005; 53:601–6. [PubMed: 15723407]
14. Streif JU, Nahrendorf M, Hiller KH, Waller C, Wiesmann F, Rommel E, Haase A, Bauer WR. In vivo assessment of absolute perfusion and intracapillary blood volume in the murine myocardium by spin labeling magnetic resonance imaging. Magn Reson Med. 2005; 53:584–92. [PubMed: 15723416]
15. Waller C, Hiller KH, Rudiger T, Kraus G, Konietzko C, Hardt N, Ertl G, Bauer WR. Noninvasive imaging of angiogenesis inhibition following nitric oxide synthase blockade in the ischemic rat heart in vivo. Microcirculation. 2005; 12:339–47. [PubMed: 16020080]
16. Vandsburger MH, Janiczek RL, Xu Y, French BA, Meyer CH, Kramer CM, Epstein FH. Improved arterial spin labeling after myocardial infarction in mice using cardiac and respiratory gated look-locker imaging with fuzzy C-means clustering. Magn Reson Med. 2010; 63:648–57. [PubMed: 20187175]
17. Hiller KH, Ruile P, Kraus G, Bauer WR, Waller C. Tissue ACE inhibition improves microcirculation in remote myocardium after coronary stenosis: MR imaging study in rats. Microvas Res. 2010; 80:484–490.
18. Qiao H, Zhang H, Zheng Y, Ponde DE, Shen D, Gao F, Bakken AB, Schmitz A, Kung HF, Ferrari VA, Zhou R. Embryonic Stem Cell Grafting in Normal and Infarcted Myocardium: Serial Assessment with MR Imaging and PET Dual Detection. Radiology. 2009; 250:821–829. [PubMed: 19244049]
19. Qiao H, Zhang H, Yamanaka S, Patel VV, Petrenko NB, Huang B, Muenz LR, Ferrari VA, Boheler KR, Zhou R. Long-Term Improvement in Postinfarct Left Ventricular Global and Regional Contractile Function Is Mediated by Embryonic Stem Cell-Derived Cardiomyocytes. Circulation: Cardiovascular Imaging. 2011; 4:33–41. [PubMed: 21059858]
20. Kober F, Iltis I, Izquierdo M, Desrois M, Ibarrola D, Cozzone PJ, Bernard M. High-resolution myocardial perfusion mapping in small animals in vivo by spin-labeling gradient-echo imaging. Magn Reson Med. 2004; 51:62–7. [PubMed: 14705046]
21. Zhou R, Pickup S, Yankeelov TE, Springer CS Jr, Glickson JD. Simultaneous measurement of arterial input function and tumor pharmacokinetics in mice by dynamic contrast enhanced imaging: effects of transcytolemmal water exchange. Magn Reson Med. 2004; 52:248–57. [PubMed: 15282806]
22. Pickup S, Wood AK, Kundel HL. A novel method for analysis of TOROM data. J Magn Reson Imaging. 2004; 19:508–512. [PubMed: 15065176]
23. Brix G, Schad LR, Deimling M, Lorenz WJ. Fast and precise T1 imaging using a TOMROP sequence. Magn Reson Imaging. 1990; 8:351–6. [PubMed: 2392022]
24. Silver MS, Joseph RI, Chen CN, Sank VJ, Hoult DI. Selective population inversion in NMR. Nature. 1984; 310:681–3. [PubMed: 6472448]

25. De Visscher G, Haseldonckx M, Flameng W. Fluorescent microsphere technique to measure cerebral blood flow in the rat. Nat Protoc. 2006; 1:2162–70. [PubMed: 17487208]
26. Eucker SA, Hoffman BD, Natesh R, Ralston J, Armstead WM, Margulies SS. Development of a fluorescent microsphere technique for rapid histological determination of cerebral blood flow. Brain Res. 2010; 1326:128–34. [PubMed: 20193669]
27. Zhou R, Pickup S, Glickson JD, Scott C, Ferrari VA. Assessment of Global and Regional Myocardial Function in the Mouse Using Cine- and Tagged MRI. Magn Reson Med. 2003; 49:760–764. [PubMed: 12652548]
28. Bogaert J, Bosmans H, Maes A, Suetens P, Marchal G, Rademakers FE. Remote myocardial dysfunction after acute anterior myocardial infarction: impact of left ventricular shape on regional function: a magnetic resonance myocardial tagging study. Journal of the American College of Cardiology. 2000; 35:1525–34. [PubMed: 10807456]
29. Zhang H, Qiao H, Bakken A, Gao F, Huang B, Liu YY, El-Deiry W, Ferrari VA, Zhou R. Utility of dual-modality bioluminescence and MRI in monitoring stem cell survival and impact on post myocardial infarct remodeling. Acad Radiol. 2011; 18:3–12. [PubMed: 21145025]
30. Detre JA, Wang J, Wang Z, Rao H. Arterial spin-labeled perfusion MRI in basic and clinical neuroscience. Curr Opin Neurol. 2009; 22:348–55. [PubMed: 19491678]
31. Kim SG. Quantification of relative cerebral blood flow change by flow-sensitive alternating inversion recovery (FAIR) technique: application to functional mapping. Magn Reson Med. 1995; 34:293–301. [PubMed: 7500865]
32. Zhang H, Qiao H, Frank R, Eucker S, Lu M, Huang B, Armstead W, Margulies S, Ferrari V, Epstein J, Zhou R. Endothelial Progenitor Cells Mediated Improvements in Post-Infarct Left Ventricular Myocardial Blood Flow Estimated by Spin Label CMR. Circulation. 2010; 122:A20415.
33. Bergmann SR, Herrero P, Markham J, Weinheimer CJ, Walsh MN. Noninvasive quantitation of myocardial blood flow in human subjects with oxygen-15-labeled water and positron emission tomography. J Am Coll Cardiol. 1989; 14:639–52. [PubMed: 2788669]
34. Wang DJ, Bi X, Avants BB, Meng T, Zuehlsdorff S, Detre JA. Estimation of perfusion and arterial transit time in myocardium using free-breathing myocardial arterial spin labeling with navigator-echo. Magn Reson Med. 2010; 64:1289–95. [PubMed: 20865753]
35. Kaufmann PA, Camici PG. Myocardial Blood Flow Measurement by PET: Technical Aspects and Clinical Applications. J Nucl Med. 2005; 46:75–88. [PubMed: 15632037]
36. Zhou R, Idiyatullin D, Moeller S, Corum C, Zhang H, Qiao H, Zhong J, Garwood M. SWIFT detection of SPIO-labeled stem cells grafted in the myocardium. Magn Reson Med. 2010; 63:1154–1161. [PubMed: 20432286]

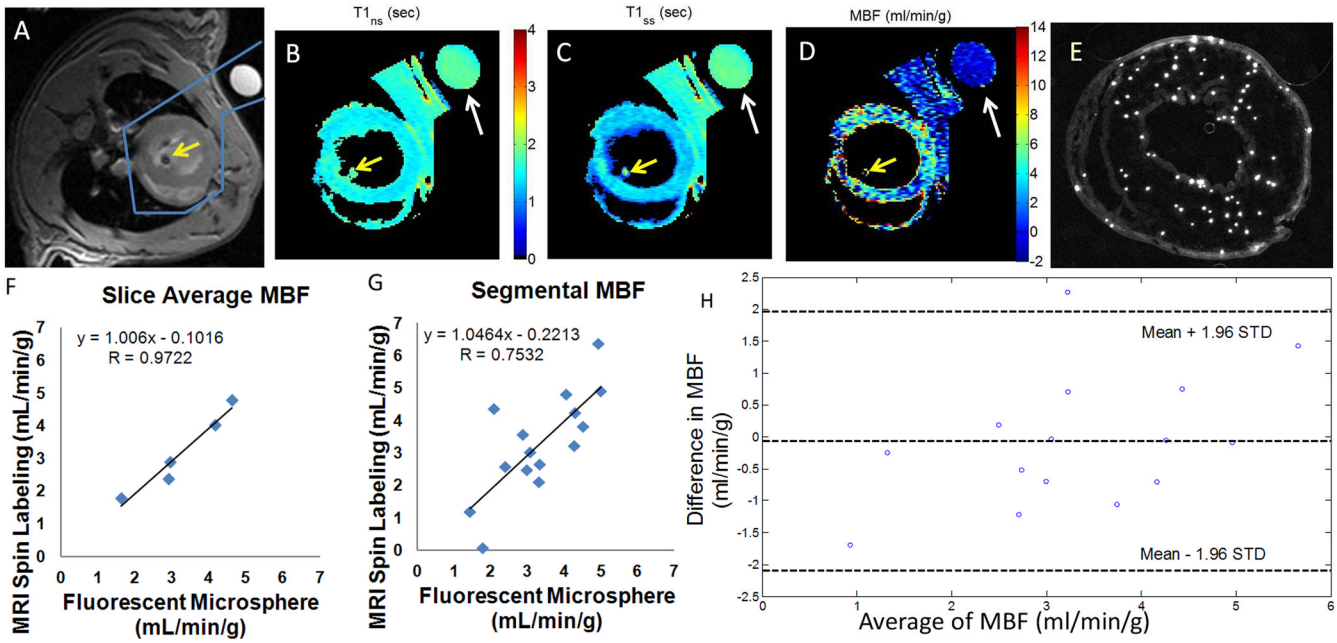

Figure 1. (A–H): Validation of SL-MRI based MBF with color microsphere technique

Non-slice selective T1 map ($T1_{ns}$, B), slice selective T1 map ($T1_{ss}$, C) and MBF map (D) calculated from the area enclosed in the blue box on the corresponding GRE image (A). White arrows point to the reference phantom while yellow arrows point to the catheter inside the LV. Distribution of FMs in a section (E). Correlation of MBF measured by SL-MRI *vs.* FM technique: average from entire slice (F) or segments (G). Myocardium wall on MBF maps and on micrographs of tissue sections was divided into 3 segments (septal, lateral, and combined anterior/posterior), resulting in 3 data points per animal × 5 animals = 15 points in G. For Bland-Altman analysis (H), the difference of MBF, (SL − FM), was plotted against the average of MBF, (SL+ FM)/2; mean difference (bias) and the 95% limits of agreement defined as bias ± 1.96 standard deviation (STD= 0.767 mL/min/g) were computed.

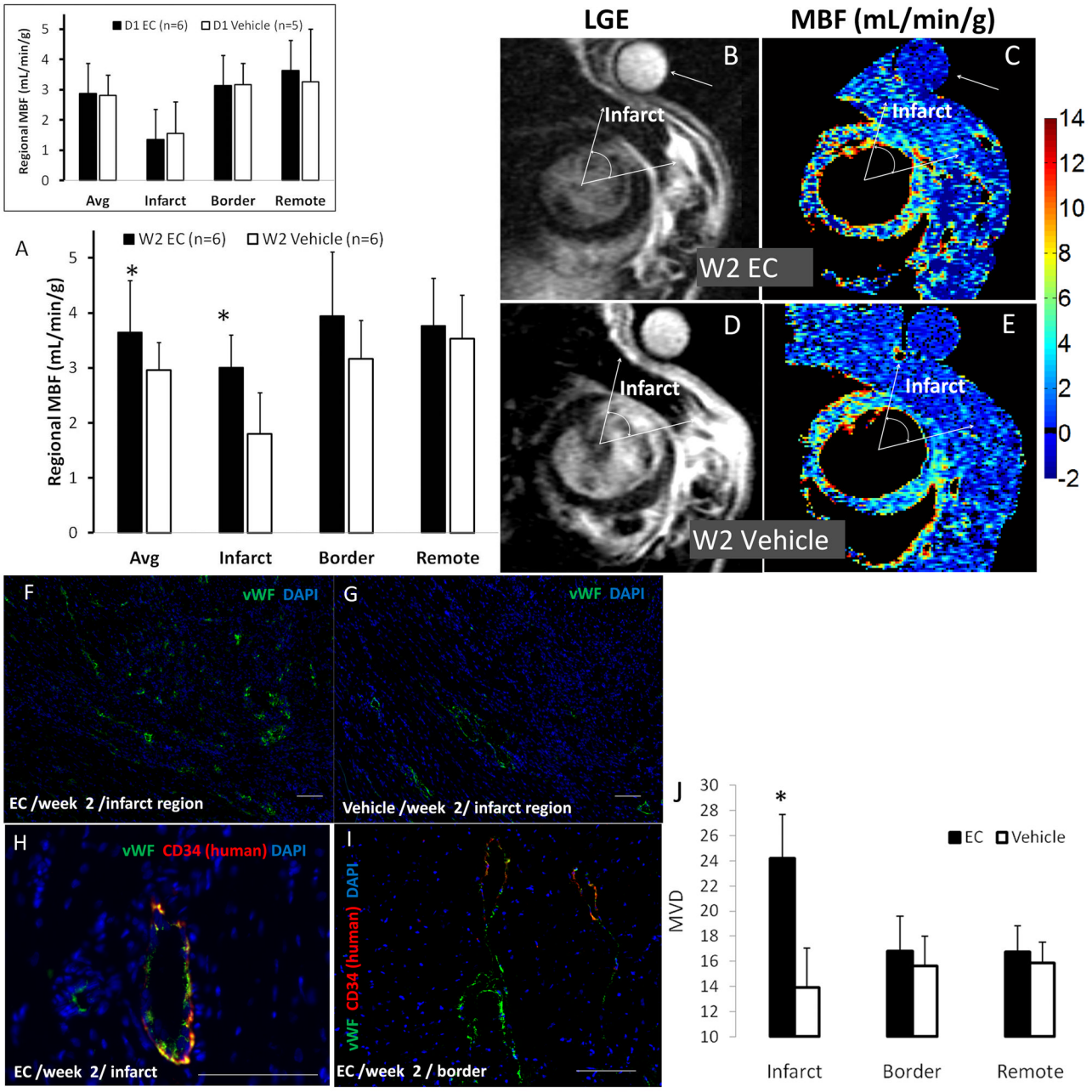

Figure 2. (A–J): Regional MBF estimated by *in vivo* MRI and MVD at 2-weeks post-MI

Slice-average and regional MBF at 1-day (inset of A) and 2-weeks post-MI (A). The MBF maps and corresponding LGE images were shown for a representative heart from EC (B–C, arrows pointing to the phantom) and Vehicle group (D–E). Immunostaining for vWF from an EC- (F) or Vehicle-treated heart (G). Double immunostaining of CD34 which reacts *only* to human tissue and vWF antibody which reacts to rat and human antigen revealed incorporation of ECs into capillaries in the infarcted (H) and border (I) region. Scale bars = 100 μm. MVD (= the number of capillaries per field of 1.1 mm^2). *: statistically significant comparing the EC *vs.* Vehicle group (A, J).

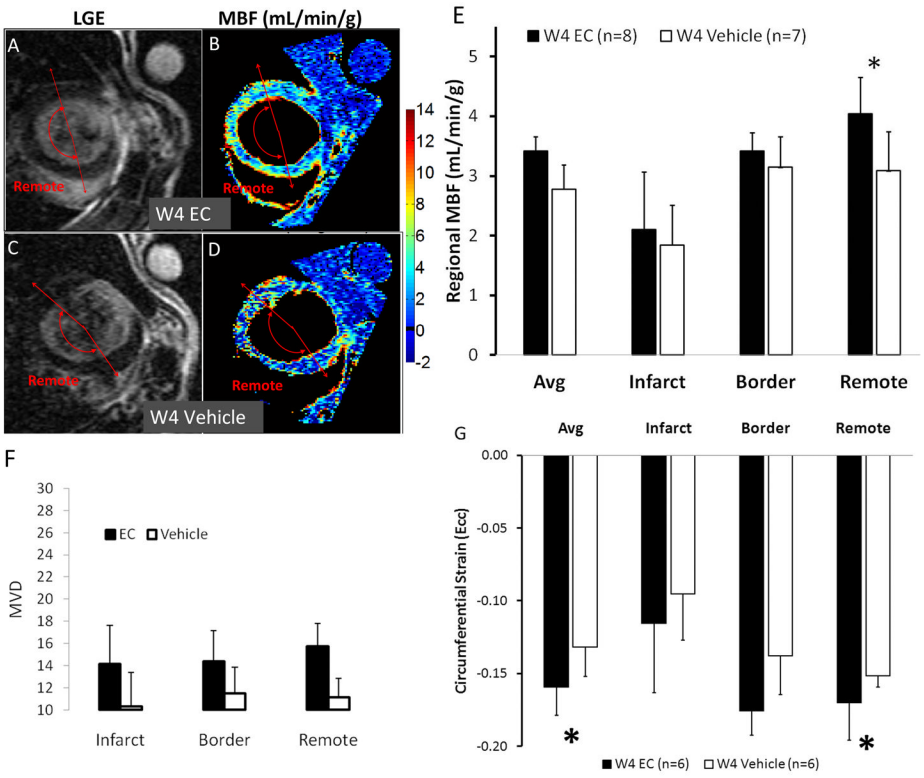

Figure 3. (A–G): Regional MBF and wall motion estimated by MRI and MVD at 4-weeks post-MI

MBF maps and corresponding LGE images were shown for a representative heart from the EC (A–B) and Vehicle group (C–D). Regional MBF (E), MVD (F) and E_{cc} (G) from the EC and Vehicle group. *: statistically significant comparing the EC *vs.* Vehicle group (E, G).

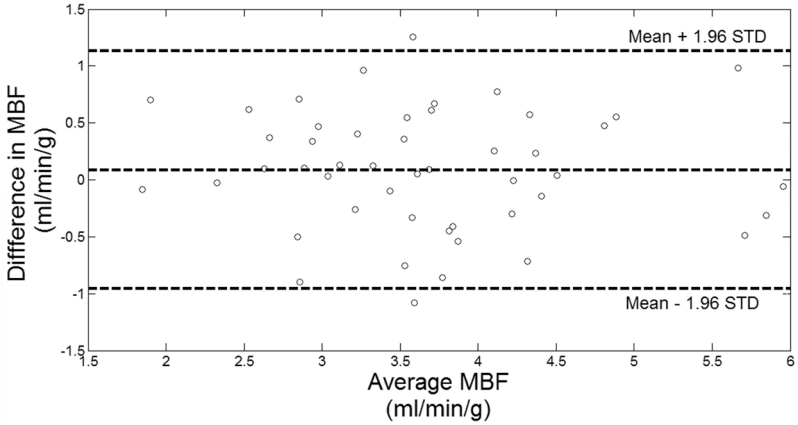

Figure 4. Blandt-Altman plot demonstrating the test-retest reproducibility of SL-MRI method

Average MBF was obtained from the septal, anterior, posterior and lateral segment for each animal. The bias between the retest and test scan is 0.088 mL/min/g with STD = 0.533 mL/min/g.

Table 1

Intraclass correlation coefficient (ICC) derived from sliced-averaged and segmental MBF

	Slice-Average	Septum	Lateral	Anterior	Posterior
Validation Study	0.975	0.624	0.946	0.708 (A/P combined)	
Reproducibility	0.913	0.850	0.711	0.635	0.889

Table 2

Cardiac and respiratory period of the animals during the validation study.

Animal	Cardiac Cycle (ms)	Respiratory Cycle (ms)
1	212 ± 15	1083 ± 169
2	210 ± 9	1071 ± 128
3	160 ± 14	723 ± 47
4	170 ± 7	1414 ± 50
5	178 ± 2	1101 ± 62

Table 3

Infarct size and global function estimated by MRI at 1 day and 4 weeks post-MI

	Day 1		Week 4	
	Infarct size[a]	**LVEF**[b]	**Infarct size**[a]	**LVEF**[b]
EC	18.3±4.7%	57.3±6.9%	4.3±2.6%	59.2±9.0%
Vehicle	16.8±5.6%	55.6±4.8%	6.2±2.6%	59.4±6.9%

a, b No statistical significance was observed between the two study groups ($p > 0.1$).